




## Research Article

# Green synthesis of silver nanoparticles using cauliflower waste and their multifaceted applications in photocatalytic degradation of methylene blue dye and Hg<sup>2+</sup> biosensing

J. Kadam<sup>1</sup> · P. Dhawal<sup>2</sup> · S. Barve<sup>2</sup> · S. Kakodkar<sup>1</sup> 

Received: 11 November 2019 / Accepted: 16 March 2020 / Published online: 21 March 2020  
© Springer Nature Switzerland AG 2020

## Abstract

Green synthesis of silver nanoparticles (AgNPs) using plant extracts has emerged as a viable environment-friendly method. The aim of the study was to biosynthesize AgNPs using cauliflower (*Brassica oleracea* var. *botrytis*) waste extract and further test their potential applications in photocatalytic degradation of methylene blue (MB) dye and Hg<sup>2+</sup> biosensing. Optimum extract concentration, AgNO<sub>3</sub> concentration, pH and temperature required for biosynthesis of stable AgNPs were determined by UV–visible spectroscopy. FT-IR, XRD, SEM, TEM, SAED, XPS and BET analysis were performed for characterizing AgNPs. MB dye degradation using AgNPs was determined by analyzing the intensity of dye absorption maxima at 664 nm. Specificity and sensitivity of biosynthesized AgNPs for Hg<sup>2+</sup> ions were studied for assessing their biosensing abilities. Optimum conditions needed for biosynthesis of stable AgNPs were observed to be 3 ml extract, 0.5 mM AgNO<sub>3</sub>, pH 8.5 and microwave-assisted heating at 600 W for 5 min. FT-IR analysis showed that the extract contained necessary functional groups that facilitated biosynthesis of AgNPs. XRD, SEM, TEM, SAED, XPS results confirmed the formation of AgNPs. BET analysis showed that AgNPs had an average size of 35.08 nm and surface area of 19.22 m<sup>2</sup>/g. Maximum MB dye degradation percentage of 97.57% was obtained at 150 min without any significant silver leaching thereby, signifying notable photocatalytic property of AgNPs. Biosensing studies showed that AgNPs were specifically able to detect up to 0.1 mg/l Hg<sup>2+</sup> ions. In summary, cauliflower waste served as a useful source of reducing agents for biosynthesizing AgNPs with promising environmental applications.

**Keywords** Silver nanoparticles · Biosynthesis · Cauliflower · Biosensor · Dye degradation

## 1 Introduction

Nanoparticles have gained immense importance in recent times due to their diverse application in the field of science and technology. By definition, they are described as microscopic particles that have size smaller than 100 nm in at least one dimension [1, 2]. Their microscopic size, morphology and distribution enable them to possess unique biological, chemical and physical properties that are distinctly different from those of individual atoms and molecules

[2, 3]. Metal nanoparticles have been extensively explored due to their diverse applications in the areas of catalysis, biosensing, medicine, drug delivery etc. [1, 4–8]. In particular, silver nanoparticles (AgNPs) have received close attention due to their unique physicochemical properties [9–12].

Colloidal silver particles have been reported to act as effective antimicrobial agents against bacteria and viruses [11, 13–15]. They also possess promising catalytic activity, which enable them to degrade harmful synthetic dyes

✉ S. Kakodkar, shrutibaadkar3@gmail.com | <sup>1</sup>Department of Biotechnology, Vinayak Ganesh Vaze College of Arts Science and Commerce, Mulund, Mumbai, Maharashtra 400081, India. <sup>2</sup>KET's Scientific Research Centre, KET's V.G. Vaze College Campus, Mulund, Mumbai, Maharashtra 400081, India.



such as methylene blue (MB), congo red, methyl orange and methyl red [2, 3, 11, 16–19]. Additionally, they have also been shown to act as efficient sensors for detecting heavy metals like mercury and copper ions [20, 21]. These AgNPs can be produced by physical, chemical and biological methods. Physical and chemical methods of synthesis pose a threat to environment due to the use of reducing and stabilizing agents that are known to be both toxic and non-biodegradable [14, 15]. Alternatively, biological synthesis or ‘Green Synthesis’ of AgNPs is considered a novel approach due to its numerous advantages such as eco-friendly nature, ease of production, feasible large-scale synthesis and lack of requirement of harmful chemical agents [9, 10, 15, 16]. Biological method essentially makes use of plant extract or microorganisms for synthesizing AgNPs. However, from the viewpoint of industrial feasibility, plant mediated green synthesis of AgNPs is considered to be more economic and safer as compared to microbe-assisted synthesis since handling and maintaining microbial cultures is often tedious [16].

Green synthesis method principally produces nanoparticles using capping and reducing agents present in plant extracts. Plant extracts can be acquired from vegetative parts such as stem, leaves, fruits, roots and flowers. These parts are rich sources of reducing agents such as membrane proteins, phenols, flavonoids and other secondary metabolites [22–24]. In addition to this, plant extracts also contain capping agents such as extracellular tannic acids, peptides and enzymes [24]. Considering the array of biomolecules present in plants, appropriate selection of suitable plant material is of utmost importance for obtaining the right combination of these agents. Several research studies have successfully synthesized AgNPs using extracts prepared from fresh plant material of *Ocimum sanctum* (Tulsi), olive leaf, *Amaranthus gangeticus* (Chinese red spinach), *Citrullus lanatus*, *Datura stramonium*, coffee, *Azadirachta indica* (neem), *Matricaria recutita* (Babunah), *Aloe vera* etc. [11, 15, 20, 21, 25–29]. Alternatively, fruit and vegetable wastes have also been utilized for synthesizing AgNPs with the purpose of curbing their overwhelming burden on the environment [24, 30–32].

Biowaste, in the form of vegetable or fruit waste, has become a major environmental concern due to its improper disposal. Among vegetables, India ranks second worldwide in cauliflower production, accounting for approximately 35% of total worldwide production [33]. Cauliflower (*Brassica oleracea* var. *botrytis*) forms an integral part of routine diet in India. As a habitual practice, cauliflower leaves are peeled off from the vegetable floret and discarded before cooking. Also, a huge amount of superfluous cauliflower leaves are removed prior to selling in vegetable markets and later dumped improperly. This improper disposal leads to unwarranted growth of harmful

microorganisms. In view of their ill effects, cauliflower and several other vegetable wastes are being extensively studied with an intention of finding their alternate applications as biofuels, compost etc. Cauliflower leaves are rich sources of polyphenols that, as mentioned above, are promising reducing agents for nanoparticle synthesis [34]. Previous research studies have synthesized AgNPs using fresh cauliflower and revealed their promising applications as antibacterial and antifungal agents against pathogens like *Escherichia coli*, *Staphylococcus aureus*, *Klebsiella Pneumoniae*, *Bacillus subtilis*, *Candida albicans* and *Aspergillus* sp. [35–37]. Another research study showed that AgNPs synthesized from fresh cauliflower floret extract display promising antioxidant and anti-cancerous properties [38]. However, till date, research on green synthesis of AgNPs using cauliflower waste and analysis of their possible environmental applications has not been explored in detail.

Therefore, in light of the above and the need for finding meaningful alternate applications of cauliflower waste, the aim of the present work was to synthesize AgNPs using extract obtained from discarded cauliflower leaves. Further, the study also assessed potential environmental applications of biosynthesized AgNPs in photocatalytic degradation of harmful MB dye and biosensing of  $Hg^{2+}$  ions.

## 2 Materials and methods

### 2.1 Preparation of cauliflower leaf waste (CLW) extract from waste *Brassica oleracea* var. *botrytis*

Discarded cauliflower (*Brassica oleracea* var. *botrytis*) leaves were collected from local market in Mumbai. These leaves were thoroughly washed with tap water and further rinsed with dechlorinated water. The washed leaves were then shade dried for 7 days and later ground using mechanical blender. Then, 10 g of dried powder was added to 100 ml dechlorinated water. The mixture was boiled for 5 min and later filtered. The filtrate obtained was used for biosynthesis of AgNPs.

### 2.2 Biosynthesis of AgNPs

For biosynthesis of AgNPs, a typical reaction mixture consisted of 3 ml of CLW extract, 1 ml of 5 mM  $AgNO_3$  and 6 ml deionised water. The solution was heated in microwave at 600 W for 5 min with intermittent mixing after which, it was further incubated in dark for 24 h. Formation of AgNPs through CLW extract mediated reduction of  $Ag^{1+}$  to  $Ag^0$  was studied by observing the color change of the reaction solution. Formation of AgNPs was also confirmed

by spectrophotometric analysis. The optical absorption of biosynthesized AgNPs was investigated at a wavelength range of 250–600 nm using Cary 50 UV–visible spectrophotometer, operated at a resolution of 1 nm.

### 2.3 Optimization of parameters

Parameters such as CLW extract concentration, AgNO<sub>3</sub> concentration, pH and temperature were optimized for biosynthesizing AgNPs. AgNO<sub>3</sub> solution and CLW extract were used as negative controls. The optimum conditions needed for successful bioreduction of silver ions and their subsequent nucleation into AgNPs were determined by spectrophotometric analysis of AgNPs after 24 h incubation in dark at room temperature.

#### 2.3.1 Concentration of CLW extract

The effect of CLW extract concentration on biosynthesis of AgNPs was studied by setting up the reaction using different volumes of CLW extract (1, 2, 3, 4 and 5 ml). The appropriate volume of extract needed for forming suitable AgNPs was determined by studying the absorption spectra of nanoparticles.

#### 2.3.2 Concentration of AgNO<sub>3</sub> solution

Optimum AgNO<sub>3</sub> concentration for nanoparticle synthesis was studied by setting up the reaction mixtures with different AgNO<sub>3</sub> concentrations (0.5, 1.0, 1.5, 2 and 2.5 mM). Optimum AgNO<sub>3</sub> concentration was determined by assessing the absorbance of nanoparticles spectrophotometrically.

#### 2.3.3 Temperature

The aforementioned reaction mixture for synthesizing AgNPs was subjected to different temperature conditions namely, microwave-assisted heating at 600 W (5 min), heating at 100 °C (1 h), and room temperature (24 h). Each reaction tube was kept at room temperature for 24 h after synthesis. The appropriate temperature condition was assessed by analyzing the absorbance spectra of these nanoparticles.

#### 2.3.4 pH

The optimum pH was studied by subjecting the standardized reaction mixture of 3 ml CLW extract, 1 ml of 5 mM AgNO<sub>3</sub> and 6 ml deionised water to different pH conditions (6.5, 7.5, 8.5, 9.5). The reaction solution was adjusted to desired pH using 0.1 N NaOH. Optimum pH was determined by studying the absorbance spectra of AgNPs.

### 2.4 Purification of AgNPs

For purification of nanoparticles, the reaction solution was centrifuged for 10 min at 10,000 rpm. The pellet obtained was washed with dechlorinated water and centrifuged at 10,000 rpm for 10 min until a clear supernatant was obtained. The washed pellet was dried overnight at room temperature. The dried AgNPs were weighed and further characterized to evaluate their shape and size.

### 2.5 Characterization of biosynthesized AgNPs

After purification, biosynthesized AgNPs were further characterized using FT-IR analysis, XRD, SEM, TEM, SAED at Sophisticated Analytical Instrumentation Facility (SAIF) at IIT Bombay. FT-IR analysis, was performed for determining the functional biomolecules in CLW extract that served as reducing and stabilizing agents for biosynthesizing AgNPs. FT-IR spectrum was recorded in the range of 3500–500 cm<sup>-1</sup> using Bruker Vertex 80, 3000 Hyperion microscope with FT-IR system. The crystalline structure of synthesized AgNPs was examined by XRD using analytical empyrean powder diffractometer with Cu K alpha radiation at 1.54184 Å. Field emission gun-scanning electron microscopy (FEG-SEM) was performed using Jeol JSM-7600F FEG-SEM for examining surface morphology of nanoparticles. Transmission electron microscopy (TEM) and selected area diffraction pattern (SAED) analysis was performed using field emission gun-TEM 300 kV for evaluating morphology and size of nanoparticles. X-ray photoelectron spectroscopy (XPS) was conducted using thermo Fischer scientific K-Alpha XPS for determining the surface chemical composition. Surface area and pore size of AgNPs was determined using BET High Speed Surface Area and Pore Size Analyzer at ICAR-CIRCOT, Mumbai.

### 2.6 Photocatalytic degradation of MB dye

Photocatalytic activity of biosynthesized AgNPs against MB dye was assessed. 5 mg of biosynthesized AgNPs was added to 50 ml of 1 mg/l MB solution. MB solution of the same concentration was used as control. Both test and control suspensions were mixed thoroughly on a shaker at 100 rpm for 30 min after which, the solutions were kept under sunlight and monitored. Next, 2 ml aliquots were removed at time intervals of 30 min till significant discoloration was observed. The aliquots were centrifuged at 10,000 rpm for 5 min. The absorbance of MB dye was measured in resultant supernatant of control and test solutions at 664 nm wavelength. Percentage of MB dye

degradation in test and control at respective time interval was calculated using the following formula:

$$\% \text{ Degradation} = 100 \times (A_0 - A) / A_0$$

where, 'A<sub>0</sub>' is the initial absorbance of MB dye solution and 'A' is the absorbance of MB dye solution obtained after each time interval. Further, the leaching of AgNPs into the solution was studied by analyzing the MB dye solution after 150 min. For this, centrifugation of the dye solution containing AgNPs was done and, the supernatant obtained was further analyzed by ICP-atomic emission spectroscopy (AES) at SAIF labs at IIT Bombay for determining the level of silver leaching that may have occurred during the photodegradation reaction.

The photocatalytic activity of biosynthesized AgNPs was evaluated by studying the degradation of phenol (5 mg/l), which is a colourless organic pollutant [39]. In the presence of sunlight, the aliquots of treated solution were taken at equal time intervals. The decrease in peak intensity of phenol at 270 nm was studied and considered to be indicative of decomposition of phenol.

The active species involved in the photocatalytic reaction were detected using trapping experiments. For this, the effect of 1 mM IPA (a quencher of •OH), 1 mM triethanolamine (a quencher of h<sup>+</sup>) and nitrogen purging (a quencher of •O<sub>2</sub><sup>-</sup>) on the photocatalytic degradation process was investigated [40]. The method employed was similar to the aforementioned photocatalytic test.

The stability and reusability of biosynthesized AgNPs were evaluated by performing a recycling study of AgNPs using earlier photocatalytic experiment. The biosynthesized AgNPs were separated after MB photodegradation reaction by centrifugation and subsequently washed using distilled water. Then, these separated AgNPs were reused in MB degradation experiment and, the percentage degradation of the dye after every cycle was determined.

## 2.7 Biosensing of Hg<sup>2+</sup> ions

### 2.7.1 Specificity

Biosynthesized AgNPs were tested as nanosensors for detecting Hg<sup>2+</sup> ions at room temperature. For demonstrating the specificity of biosynthesized AgNPs for Hg<sup>2+</sup> ions, AgNPs were tested against various metal ions such as Hg<sup>2+</sup>, Co<sup>2+</sup>, Pb<sup>2+</sup>, Mn<sup>2+</sup>, Mg<sup>2+</sup>, Zn<sup>2+</sup>, Ni<sup>2+</sup>, Na<sup>+</sup>, K<sup>+</sup>, Ba<sup>2+</sup>, Cu<sup>2+</sup>, Al<sup>3+</sup> and Fe<sup>3+</sup>. For this, 1 ml aliquot of 20 mg/l salt solution was treated with 100 µl of as-synthesized AgNPs. A solution of 100 µl of as-synthesized AgNPs in 1 ml distilled water was used as control. Control and test solutions were allowed to stand at room temperature for 10 min. The results were

visually analyzed by comparing the colour of test solution to that of the control.

### 2.7.2 Sensitivity

AgNPs were further tested to determine their limit of detection for Hg<sup>2+</sup> ions. To demonstrate this, different concentrations of HgCl<sub>2</sub> solutions (20 mg/l, 1 mg/l, 0.1 mg/l, 0.01 mg/l, 0.001 mg/l) were treated with 100 µl of as-synthesized AgNPs. After 10 min incubation at room temperature, the solutions were visually analyzed for any colour change and, their absorption spectra were studied between 250 and 600 nm wavelength using a spectrophotometer.

## 3 Results and discussion

### 3.1 Optimization of parameters for biosynthesis of AgNPs

Green synthesis of nanoparticles has emerged as a novel approach in the field of nanotechnology due to its ability to provide effective control over growth and stabilization of nanocrystals [41]. Several research studies have used the green approach for synthesizing AgNPs in order to address the problem of environmental pollutants and harmful microorganisms. For this, such studies have majorly relied and proven the potential use of fresh plants as a reducing source for nanoparticle synthesis. However, the practical applicability of such systems on a large scale entails using large quantities of fresh plant material and this, can in turn inadvertently impact the ecosystem balance. Alternatively, lab scale culturing of such fresh plants for availing their growth and use in nanoparticle synthesis is also tedious. In view of this, it is advisable to rely on the readily available large amount of bio-waste for obtaining useful nanoparticles. In the current study, cauliflower vegetable waste was used for biosynthesizing AgNPs. The present study employed the idea of 'waste to wealth' and tested nanoparticle synthesis as an alternative method for converting cauliflower waste to useful AgNPs.

It is known that plant extract concentration, AgNO<sub>3</sub> concentration, pH, and temperature are some of the defining factors that affect the rate of synthesis of nanoparticles and their quality [9]. Hence these parameters were optimized to obtain AgNPs of desired size and morphology. During standardization, the initial assessment of nanoparticle formation was done by observing the colour change of the solution. The CLW extract imparted a characteristic yellow colour. Interestingly, reaction between AgNO<sub>3</sub> and extract led to a change in colour from yellow to reddish brown. This may be attributed to the surface plasmon



resonance (SPR) of biosynthesized AgNPs [42]. Optimum parameters for biosynthesis of AgNPs were further confirmed by studying their SPR absorption band since it provides vital information regarding size and number of nanoparticles formed [9, 42].

The first parameter considered for standardization was concentration of CLW extract. All reaction tubes displayed a distinct colour change from yellow to reddish brown. It was further observed that lower extract concentration (1 ml and 2 ml) did not yield a prominently sharp absorption peak (Fig. 1). However, when the volume of the extract was increased to 3 ml, a sharp peak was noted at 422 nm wavelength. This may be attributed to the formation of small sized AgNPs. Further increase in extract concentration to 4 ml and 5 ml caused the absorption peak to shift to 436 nm and 445 nm respectively. These peaks also exhibited evident broadening thereby, suggesting an increase in nanoparticle size. Higher concentration of CLW extract provides more reducing agents that might abruptly accelerate the process of nucleation and affect the growth of nanoparticles [43]. Based on these results, 3 mL CLW extract was considered optimum for producing desired AgNPs.

The next factor considered for optimization was  $\text{AgNO}_3$  concentration (Fig. 2). For this,  $\text{AgNO}_3$  concentrations ranging from 0.5 to 2.5 mM were considered. AgNPs synthesized using 0.5 mM  $\text{AgNO}_3$  showed sharp absorption peak at 424 nm (Fig. 2). It was further observed that the peak shifted to wavelengths 445 nm and 437 nm in the reaction system containing 1.0 mM and 1.5 mM  $\text{AgNO}_3$  respectively. Also, further increase in  $\text{AgNO}_3$  concentration to 2.0 mM and 2.5 mM yielded AgNPs that displayed broad peaks at 424 nm and 408 nm respectively. Based on these findings, 0.5 mM  $\text{AgNO}_3$  was considered as the optimum concentration for biosynthesizing AgNPs.

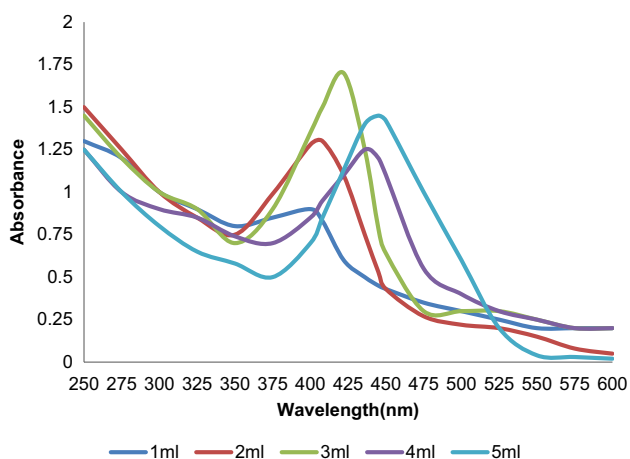


**Fig. 1** UV-visible spectra of biosynthesized AgNPs at different CLW extract concentration (1 ml, 2 ml, 3 ml, 4 ml, 5 ml)

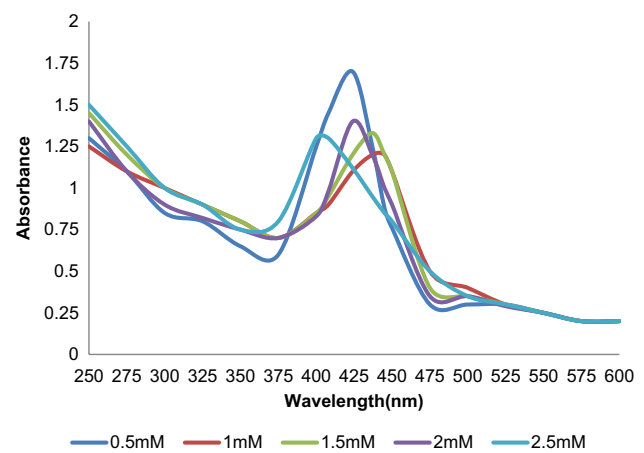


**Fig. 2** UV-visible spectra of biosynthesized AgNPs at different  $\text{AgNO}_3$  concentration (0.5 mM, 1.0 mM, 1.5 mM, 2.0 mM, 2.5 mM)

The third parameter considered for optimization was temperature (Fig. 3). There was no characteristic colour change observed in the reaction system incubated at room temperature. Also, UV-visible spectral analysis of this system, displayed no significant peak in the wavelength range of 400–500 nm (Fig. 3). AgNPs synthesized at 100 °C displayed broad SPR absorption band at 421 nm. On the other hand, AgNPs synthesized by microwave assisted heating produced sharp absorption peak at 411 nm. Microwave mediated synthesis, as compared to conventional heating, facilitates rapid heating and facilitates nucleation of metal nanoparticles thereby, aiding in nanoparticle synthesis [44]. Thus, due to favourable kinetics and rapid nanoparticle synthesis, microwave assisted heating was considered as the preferred condition for producing AgNPs in the current study.

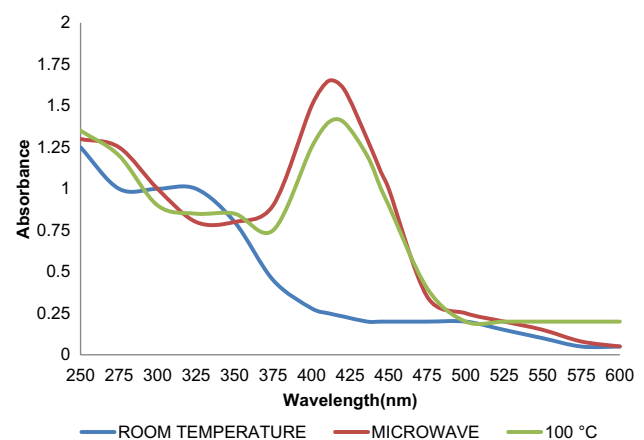


**Fig. 3** UV-visible spectra of biosynthesized AgNPs at different temperature conditions (room temperature, microwave 600 W, 100 °C)

The final parameter considered for optimization was pH. pH influences nanoparticle synthesis by altering the charges of biomolecules [45]. Owing to the charge alteration, nanoparticle synthesis is suppressed at acidic pH and enhanced at alkaline conditions [9]. In the present study, the unaltered pH of the reaction mixture was 5.5. At this pH, SPR band of biosynthesized AgNPs was observed at 445 nm (Fig. 4). Increase in pH of the reaction system to 6.5 displayed evident absorption band broadening. Further increase in pH to 7.5 and 8.5 caused spectral shift of SPR absorbance band to 425 nm and 411 nm respectively. However, the absorption peak obtained at pH 7.5 was noted to be broad in size. On the other hand, a sharp narrow peak was seen at pH 8.5, indicating synthesis of small sized AgNPs. Further increase in pH to 9.5 led to a decrease in the absorbance intensity and peak broadening at 411 nm. Based on these findings, pH 8.5 was considered optimum for biosynthesis of AgNPs. Based on the above results, the optimized reaction parameters considered for biosynthesizing AgNPs were: 3 ml CLW extract, 0.5 mM AgNO<sub>3</sub>, pH 8.5 and microwave assisted heating at 600 W for 5 min. These biosynthesized AgNPs were observed to be stable for one month when stored at room temperature.

### 3.2 FT-IR analysis

FT-IR analysis was performed to detect functional groups of biomolecules in CLW extract that may be responsible for reducing silver ions. The FT-IR spectra of CLW extract showed prominent absorption bands at 3404.74 cm<sup>-1</sup>, 1622.51 cm<sup>-1</sup>, 1508.12 cm<sup>-1</sup>, 1410.99 cm<sup>-1</sup> and 1078.93 cm<sup>-1</sup> (Fig. 5a). 3404.74 cm<sup>-1</sup> and 1622.51 cm<sup>-1</sup> correspond to O–H stretching in carboxyl and amino groups present in amino acids and stretching vibrations of

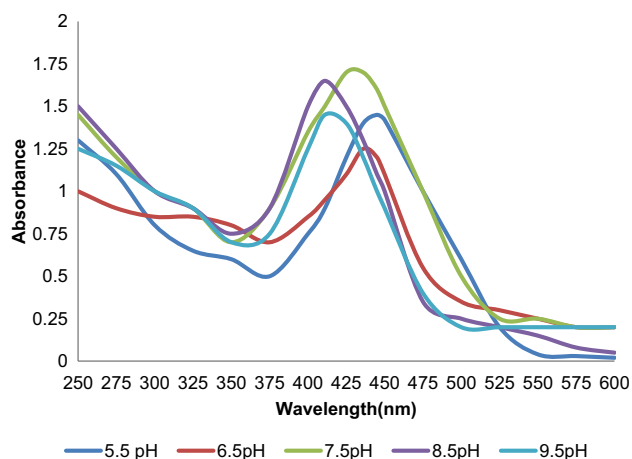


**Fig. 4** UV-visible spectra of biosynthesized AgNPs at different pH (5.5-unaltered, 6.5, 7.5, 8.5, 9.5)

aliphatic C=C group respectively [46, 47]. The absorption band at 1508.12 cm<sup>-1</sup> represent amide II in protein [48]. The absorption band at 1410.99 cm<sup>-1</sup> represent stretching vibrations of C=O groups in aromatic rings [46]. On the other hand, absorption peak at 1078.93 cm<sup>-1</sup> are due to ether linkages that may be contributed by flavanones present in the extract [49].

It was observed that purified AgNPs spectra showed shift in the peaks along with reduced absorption band intensities at 3452.60 cm<sup>-1</sup>, 1638.61 cm<sup>-1</sup>, 1601.59 cm<sup>-1</sup> and 1411.60 cm<sup>-1</sup> (Fig. 5b). These results indicate that –OH functional group, aliphatic C=C and C=O groups in aromatic rings could be the contributing factor aiding in reduction of silver and stabilization of AgNPs. Additionally, FT-IR spectra of AgNPs also revealed disappearance of absorption bands previously observed in CLW extract at 1508.12 cm<sup>-1</sup> and 1078.93 cm<sup>-1</sup> indicating that functional groups in proteins and flavonoids could also be the possible attributing factors. FT-IR spectra of AgNPs also displayed additional low intensity peaks at 2926.27 cm<sup>-1</sup>, 2854.65 cm<sup>-1</sup>, 1036.39 cm<sup>-1</sup> and 1008.24 cm<sup>-1</sup> that correspond to C–H bond stretching, bending vibrations of C–OH and C–O bonds respectively [17, 46]. These reducing functional groups have been reported to facilitate formation of stable metal nanoparticles due to their strong affinity towards metal ions. The current findings thus suggest that CLW extract possesses the necessary functional groups required for mediating biosynthesis of stable AgNPs.

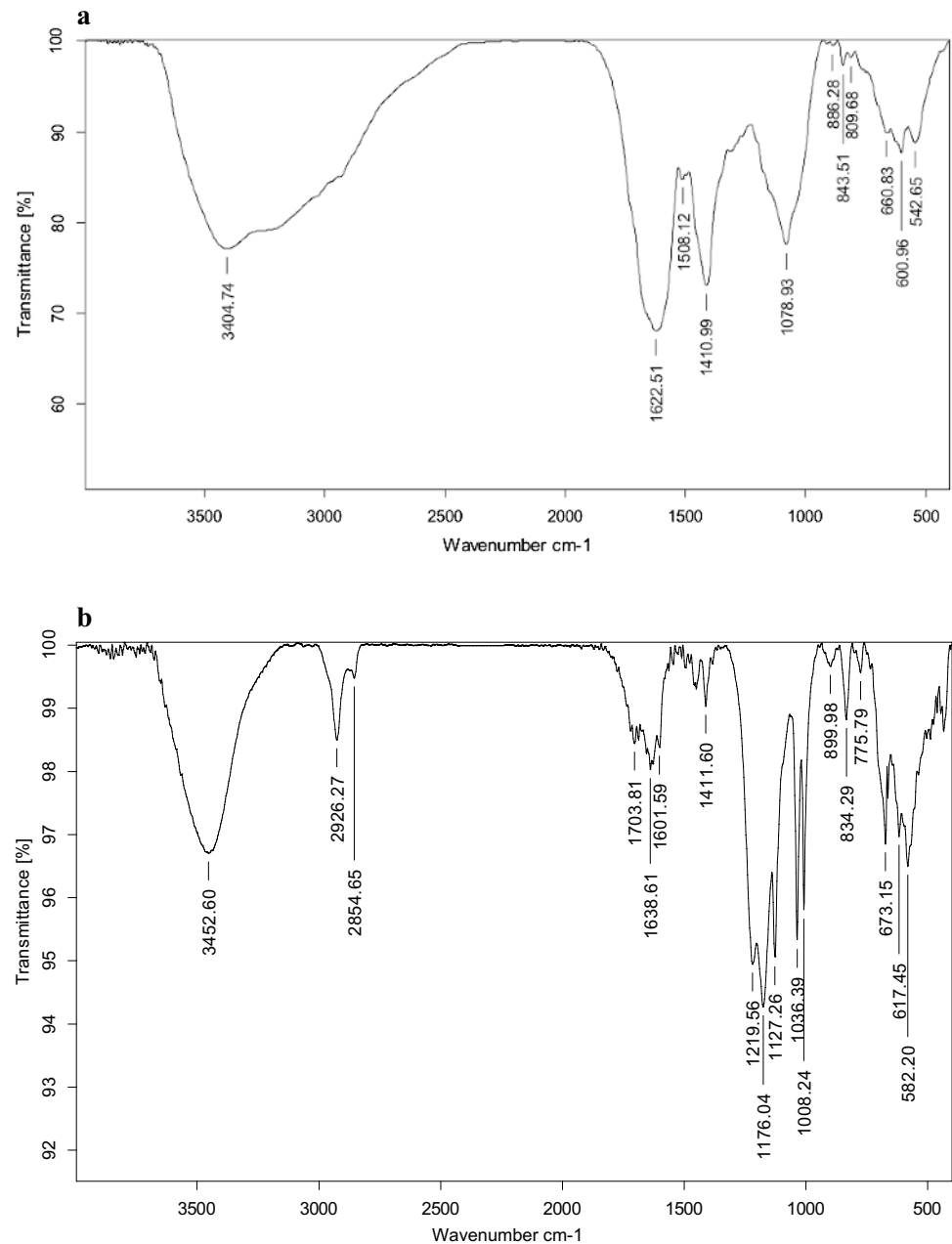
### 3.3 XRD analysis

Crystalline nature of biosynthesized AgNPs was studied using XRD analysis. The Bragg's reflection was observed at 38.4°, 44.3°, 64.2° and 77.3° and indexed at 111, 200, 220, and 311 facets of the face centred cubic crystal (fcc) structure. These values agree well with those reported for silver (face centre cubic structure) by joint committee on powder diffraction standards, File No. 04-0783. On further substituting the wavelength value of 1.5404 Å in Scherrer's formula  $D = (0.9 \lambda \times 180^\circ) / \beta \cos \theta$ , the average grain size of biosynthesized AgNPs was found to be 10 nm. The XRD data confirms that biomolecules in CLW extract reduced silver ions to silver metal.

### 3.4 FEG-SEM analysis

Shape and surface morphology of biosynthesized AgNPs was assessed by FEG-SEM analysis. The surface morphology of biosynthesized AgNPs indicated that they were predominantly even shaped and spherical in nature (Fig. 6).

**Fig. 5** **a** FT-IR spectra of CLW extract. **b** AgNPs synthesized using CLW extract



### 3.5 TEM and SAED pattern study

TEM analysis revealed the spherical morphology of bio-synthesized AgNPs (Fig. 7a). The size of nanoparticles ranged between 5 and 50 nm (Fig. 7b). The crystalline nature of AgNPs was studied by SAED pattern analysis. The results of SAED analysis were in agreement with that of XRD. The characteristic diffraction rings were indexed as (111), (200), (220) and (311) which are consistent with fcc lattice structure typically observed for AgNPs.

### 3.6 XPS analysis

Figure 8 displays XPS spectrum of AgNPs in the range of 0–1300 eV. The spectrum revealed high resolution XPS signal of Ag 3d region confirming the presence of Ag. The Ag 3d region displayed characteristic peaks at 374.08 eV and 368.08 eV which are attributed to Ag 3d<sub>3/2</sub> and Ag 3d<sub>5/2</sub> orbits of metallic silver [50]. A peak at 284.68 eV was noted in C(1s) spectrum corresponding to C–O bond which is in accordance with the above FT-IR results [51]. The O(1s)



**Fig. 6** SEM image displaying spherical shape of biosynthesized AgNPs

region displayed an intensity at binding energy 532.68 eV which also corresponds to the interaction between carbon and oxygen in C–O bond [52]. Thus, the above XPS results provide strong evidence of presence of metallic Ag in our biosynthesized nanoparticles.

### 3.7 BET analysis

BET analysis of AgNPs was conducted for determining average size, surface area and pore size of nanoparticles [53]. The surface area and average pore radius of biosynthesized AgNPs were found to be 19.22 m<sup>2</sup>/g and 7.1 nm respectively. Considering that the nanoparticles were found to have spherical shape in TEM-imaging, BET results were further used to calculate average equivalent particle size by using the equation  $D_{\text{BET}} = 6000 / (\rho S_w)$  (in nm) where,  $D_{\text{BET}}$  is the average diameter of a spherical particle,  $S_w$  represents obtained surface area of the powder in m<sup>2</sup>/g, and  $\rho$  is the theoretical density in g/cm<sup>3</sup> [54]. The analysis revealed the average nanoparticle size to be 35.08 nm. Table 1 displays BET experimental results of biosynthesized AgNPs. The  $D_{\text{BET}}$  nanoparticle size value was found to be within the range obtained using TEM-SAED imaging.

### 3.8 Photocatalytic degradation of MB dye

Synthetic dyes are commonly used in textiles, paper, adhesives, cosmetics, food, ink, medicines etc. [3]. MB is a heterocyclic azo dye which is commonly released through the effluents of textile industries. It depletes oxygen from the surface of water bodies which in turn affects aquatic flora and fauna. In addition to being an environmental hazard, it is also known to cause toxicity in humans [3]. Hence,

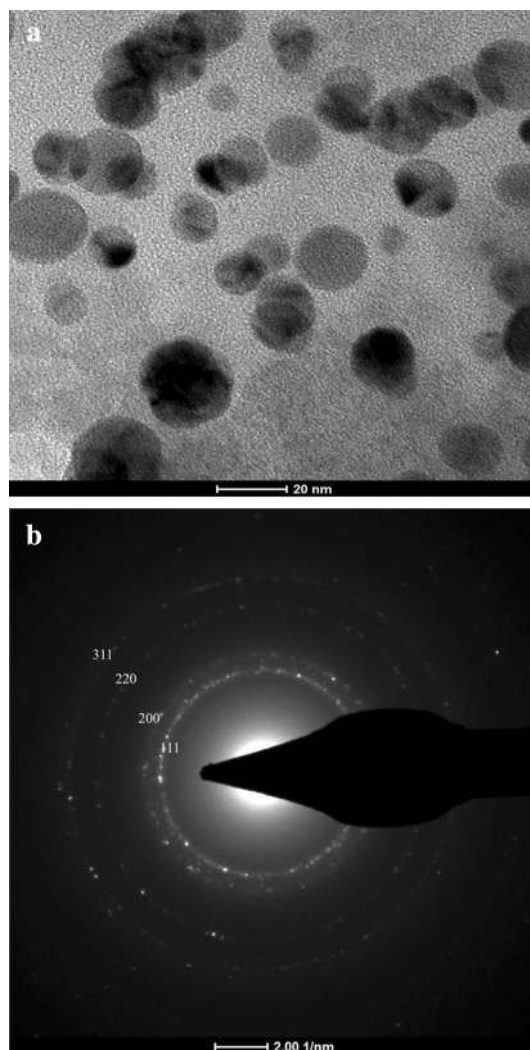


**Fig. 7** **a** TEM image of biosynthesized AgNPs. **b** SAED pattern of biosynthesized AgNPs

degradation of MB dye in effluents is highly warranted in order to eradicate its deleterious effects. AgNPs of appropriate size and shape possess high surface area to volume ratio that enable them to act as excellent catalysts in dye degradation [17–19]. The current study investigated the potential photocatalytic activity of biosynthesized AgNPs against MB. MB solution underwent visible colour change on addition of nanoparticles. Initially, the colour of MB solution was deep blue which later turned dark green on addition of AgNPs. Subsequently, under sunlight exposure, the intensity of dark green colour further reduced with increase in time. The extent of degradation of MB using biosynthesized AgNPs was monitored by UV–visible spectrophotometer. The absorption maxima for MB was found to be centred at 664 nm wavelength. The control MB solution which was also exposed to sunlight showed no significant colour change and MB degradation (Table 2).



**Fig. 8** XPS spectrum: Ag 3d peak scan

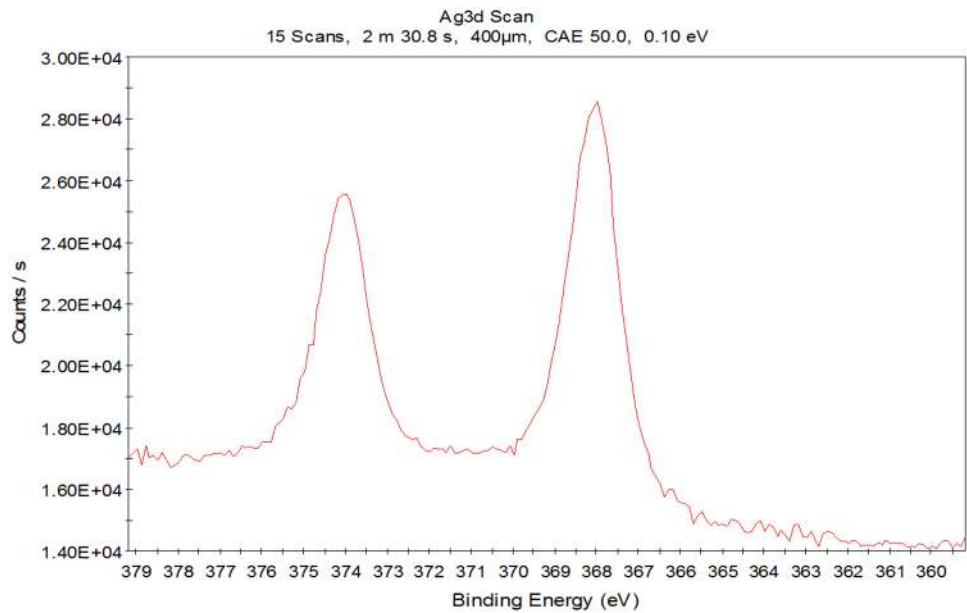


**Table 1** BET results of biosynthesized AgNPs

Sample	BET surface area (m <sup>2</sup> /g)	Average pore radius (nm)	Cumulative pore volume of pores (cm <sup>3</sup> /g)	Average particle size D <sub>BET</sub>
Ag-Np	19.22	7.1	6.827 × 10 <sup>-2</sup>	35.08 nm

**Table 2** Percentage degradation of MB dye

Time interval (min)	MB dye degradation (%)	
	Control	Test
0	-	-
30	6.31	36.89
60	9.71	44.17
90	9.71	75.24
120	9.71	87.38
150	9.71	97.57

Control: MB dye solution  
 Test: MB dye solution + biosynthesized AgNPs

However, in the presence of AgNPs, a reduction in MB absorption band was noted with increase in time (Fig. 9). Maximum photocatalytic degradation of MB was assessed by noting the time required for the MB absorption band to approach the baseline. Based on this principle, the maximum percentage of nanoparticle-mediated MB dye degradation was found to be 97.57% at 150 min (Table 2).

Kinetic parameters and correlation coefficients are presented in Table 3. Linear regression of  $\ln(C/C_0)$  (where, C = concentration of dye at time (t) and C<sub>0</sub> = concentration

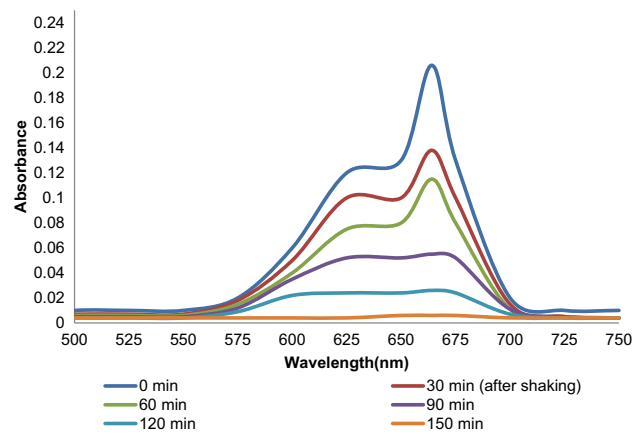


**Fig. 9** UV-visible spectra of methylene blue dye in the presence of biosynthesized AgNPs at different time intervals

**Table 3** Summary of kinetic parameters of degradation reaction of MB dye

Reaction	K (min <sup>-1</sup> )	t <sub>1/2</sub> (min)	R <sup>2</sup>
No AgNPs	0.00265	261.5	0.84540
AgNPs	0.02308	30.0	0.89926

of dye at time 0 h) confirmed pseudo-first order nature of reduction of MB dye in presence of AgNP catalyst (Fig. 10). As seen in the table, the photodegradation reaction occurred almost 9 times faster in presence of AgNPs thereby, highlighting its significance in dye degradation. AES results showed that MB dye solution alone without AgNPs contained 0.013 mg/l Ag<sup>+</sup>. The supernatant

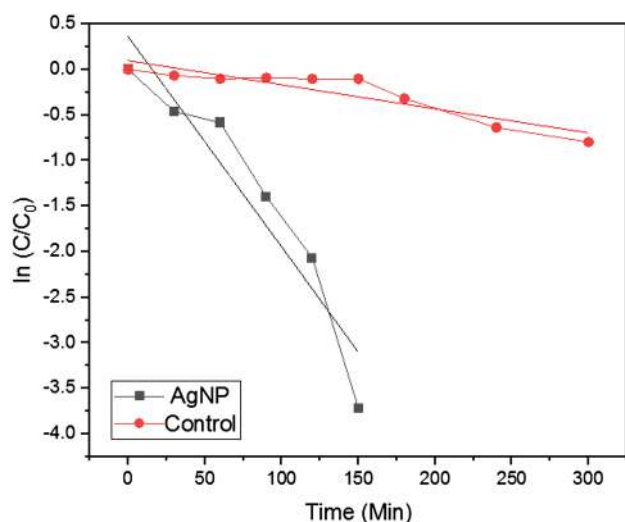


**Fig. 10**  $\ln(C/C_0)$  versus time (min) plot for the photodegradation of MB dye

obtained after maximum MB degradation using AgNPs contained 0.103 mg/l of  $\text{Ag}^+$ , thereby indicating an increase of 0.09 mg/l  $\text{Ag}^+$  ions in the solution. However, it should also be noted that this observed increase in silver ions in the solution after the reaction is well within its permissible limit in water (0.1 mg/l) as per the guidelines recommended by the World Health Organization (WHO). Table 4 highlights previous research done on MB dye degradation using AgNPs as photocatalyst in the presence of sunlight. Based on these findings, it can be concluded that our biosynthesized AgNPs can act as efficient photocatalyst in MB dye degradation without causing any significant silver leaching. However, further studies assessing the ability of these AgNPs in degrading MB in industrial effluent samples are warranted to further corroborate the current findings.

Further, the study used phenol as a colourless organic pollutant for proving that the fading of MB dye was due to photodegradation and not dye sensitization. The

UV-visible spectrum of phenol was studied for evaluating its degradation under sunlight in the presence of biosynthesized AgNPs. The absorption band of phenol at 270 nm decreased in the presence of AgNPs, whereas no change in absorption spectrum was noted in the control phenol solution without AgNPs (Fig. 11 a, b). This nanoparticles mediated prominent reduction in phenol confirms that AgNPs facilitate photocatalytic degradation.

Active species trapping experiment was performed for determining the mechanism of observed photodegradation (Fig. 12 a, b). The addition of IPA resulted in significant decrease in photocatalytic degradation wherein, only 22.56% of MB was degraded after 150 min. Addition of triethanolamine to the reaction mixture caused a dye reduction of 63.03%. Conversely, deoxygenation of MB solution resulted in negligible change in the degradation. This suggests that hole ( $h^+$ ) and hydroxyl  $\cdot\text{OH}$  radical act as main active species in the photodegradation process of MB dye using our biosynthesized AgNPs. Based on these observations, the possible mechanism of photodegradation is proposed in Fig. 12b. When the MB dye and AgNP system is irradiated with sunlight, electrons in the valance bond (VB) are excited to conduction bond leading to same number of holes ( $h^+$ ) in the VB. The photo-generated electrons in the catalyst are captured by  $\text{O}_2$  leading to formation of  $\cdot\text{O}_2^-$ , which in turn forms  $\text{OH}^-$  and further oxidize MB dye to form  $\text{CO}_2$  and  $\text{H}_2\text{O}$ . On the other hand,  $h^+$  holes react with existing  $\text{OH}^-$  to form  $\text{OH}^\cdot$  which in turn aids in photodegradation of the dye. However, in the current system the photo-induced  $\cdot\text{OH}$  are suggested to play the most vital role in photodegradation of MB dye as maximum inhibition of dye degradation was observed in the reaction system containing its quencher i.e. IPA.

The results of photodegradation of MB dye using recycled AgNPs for every run are displayed in Fig. 13. The recycled AgNPs demonstrated good photocatalytic activity up to four successive cycles. However, it was noted that the time required for attaining maximum MB degradation increased with each cycle. Based on these results, it can be

**Table 4** Comparison of results of current study with previously reported data on AgNP mediated photocatalytic degradation of MB dye in presence of sunlight

Reducing agent for AgNP synthesis (extract)	MB dye Conc (mg/l)	AgNPs (mg/l)	Reducing agent	% Degradation	Time required	References	Leaching
<i>Casuarina equisetifolia</i>	1	100	Sunlight	35–40	300 min	[2]	–
<i>Morinda tinctoria</i>	10	100	Sunlight	95.3	72 h	[16]	–
Pomegranate Peel	10	100	Sunlight	89	48–72 h	[55]	–
<i>Durio Zibethinus seed waste</i>	10	100	Sunlight	73.49	180 min	[56]	–
<i>Ageratum conyzoides</i>	10	200	Sunlight	100	105 min	[57]	–
<i>Gymnema Sylvestre</i>	10	100	Sunlight	95	420 min	[58]	–
Cauliflower leaf waste	1	100	Sunlight	97.57	150 min	Present study	0.09 mg/L

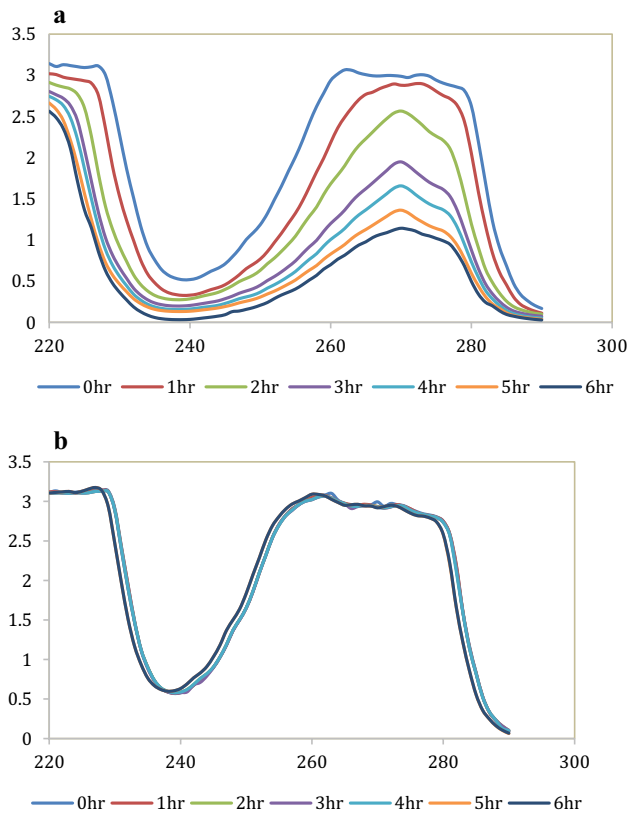


**Fig. 11** **a** UV-visible spectra of phenol in presence of biosynthesized AgNPs. **b** UV-visible spectra of phenol in absence of AgNPs

concluded that our biosynthesized AgNPs act as efficient photocatalyst with good stability and reusability. These AgNPs can be recycled for long-term application in the degradation of MB dye.

### 3.9 Biosensing of Hg<sup>2+</sup> ions

Mercury ions are considered to be one of the most toxic heavy metal ions that can severely impact human health and other living organisms. Several conventional detection methods are used for detecting Hg<sup>2+</sup> ions such as inductive coupled plasma mass spectrometry, atomic absorption spectroscopy, fluorescent sensors and electrochemical methods [59–62]. However, these techniques face limitations due to their cost, time-consuming sample preparation and complex experimental procedures [63]. Alternatively, simpler methods such as colorimetric assays have gained immense attention due to their simple and rapid principle of Hg<sup>2+</sup> detection [63, 64]. Amongst these,

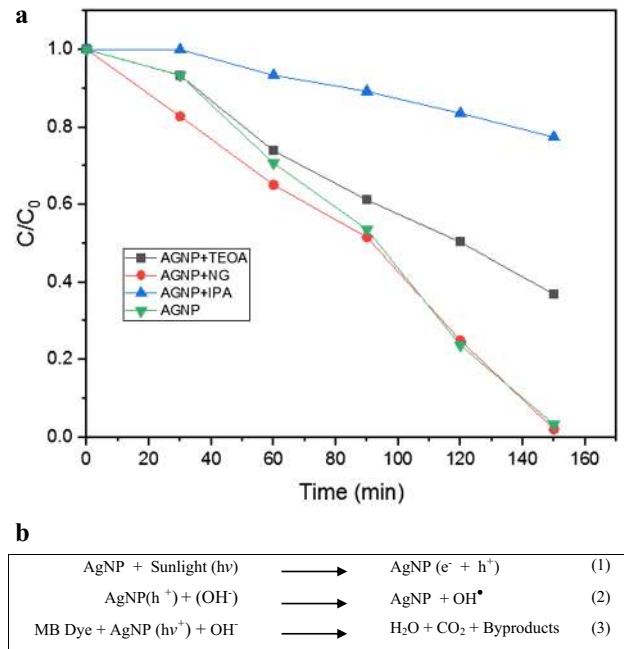


**Fig. 12** **a** Effect of different radical scavengers on the photocatalytic degradation of MB dye using biosynthesized AgNPs. **b** Possible photocatalytic mechanism of biosynthesized AgNPs in degradation of MB dye

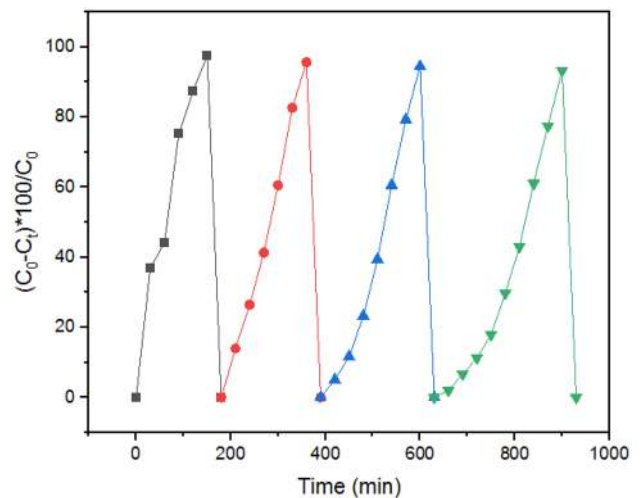


**Fig. 13** Reusability of biosynthesized AgNPs in MB dye degradation. (1st cycle-black, 2nd cycle-red, 3rd cycle-blue, 4th cycle-green)

silver and gold nanosensor based colorimetric assays are considered promising owing to their unique physicochemical properties. However, AgNPs are considered to be more

**Fig. 14** Image displaying reaction between various metal ions and as-synthesized AgNPs

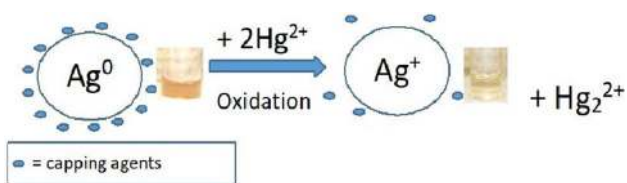
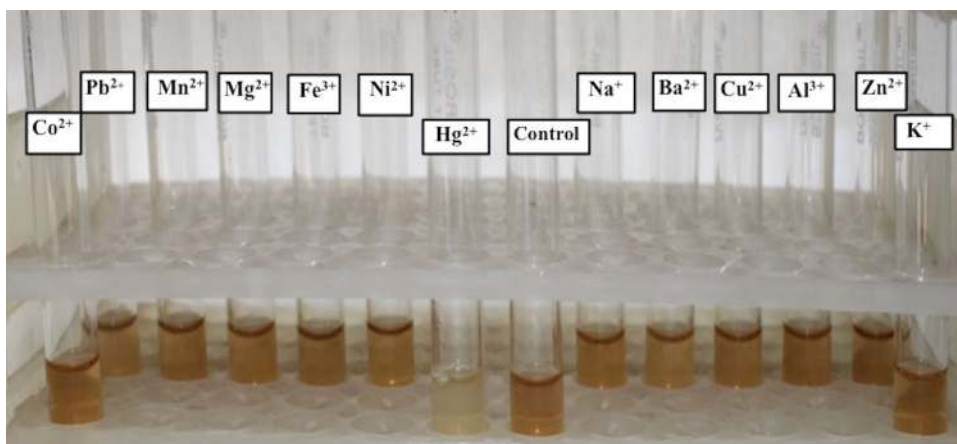


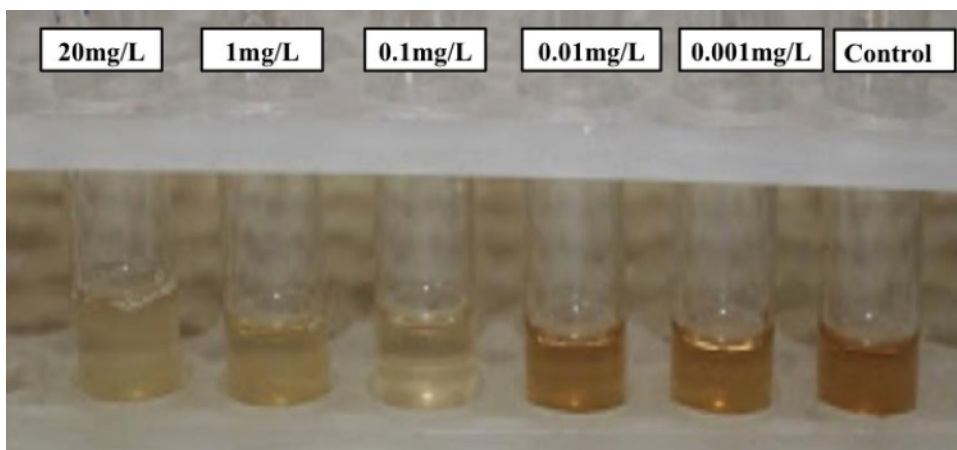
**Fig. 15** Schematic illustration of mercury sensing

effective as sensors as compared to gold nanoparticles due to their cost-effectiveness and high extinction coefficients [64].

In view of this, the present study evaluated the possible application of as-synthesized AgNPs as biosensors for Hg<sup>2+</sup> detection. The specificity of as-synthesized AgNPs

for Hg<sup>2+</sup> was studied by noting their reaction with other metal cations such as, Co<sup>2+</sup>, Pb<sup>2+</sup>, Mn<sup>2+</sup>, Mg<sup>2+</sup>, Zn<sup>2+</sup>, Ni<sup>2+</sup>, Na<sup>+</sup>, K<sup>+</sup>, Ba<sup>2+</sup>, Cu<sup>2+</sup>, Al<sup>3+</sup>, Fe<sup>3+</sup> in addition to Hg<sup>2+</sup> ions. It was found that colour of the reaction mixture of Hg<sup>2+</sup> ions and as-synthesized AgNPs changed from brown to pale yellow (Fig. 14). This colour change may be attributed to the redox reaction between zero valent silver and divalent mercury ions. A probable mechanism of interaction between AgNPs and Hg<sup>2+</sup> has been proposed in (Fig. 15). Upon interaction of Hg<sup>2+</sup> solution with as-synthesized AgNPs, decrease in the absorbance intensity was noted due to redox reaction between silver and mercury ions leading to aggregation and Ag-Hg amalgam formation [65]. Redox reaction happens due to the fact that standard reduction potential of Hg<sup>2+</sup>/Hg (0.85 V) is higher than that of Ag<sup>+</sup>/Ag (0.80 V) [66]. Thus, oxidation of Ag<sup>0</sup> to Ag<sup>1+</sup> (of

**Fig. 16** Image displaying reaction between different concentrations of Hg<sup>2+</sup> ions (20 mg/l, 1 mg/l, 0.1 mg/l, 0.01 mg/l, 0.001 mg/l) and as-synthesized AgNPs





AgNPs) changes the colour of the reaction solution from brown to pale yellow. In contrast, no colour change was observed when as-synthesized AgNPs were added to other metal ion solutions. Most of the transition metals, alkali and alkali earth metals cannot oxidize  $\text{Ag}^0$  to  $\text{Ag}^{1+}$  as their standard reduction potential are lower than that of  $\text{Ag}^+/\text{Ag}$  [66]. These results show that the colorimetric sensor method developed using as-synthesized AgNPs is highly specific for  $\text{Hg}^{2+}$  ions.

Considering the specificity results, we further evaluated the sensitivity of our silver nanosensors for  $\text{Hg}^{2+}$  ions. For this, varied concentrations of  $\text{Hg}^{2+}$  solutions were tested with as-synthesized AgNPs. UV-visible spectral analysis was carried out for studying the interaction between  $\text{Hg}^{2+}$  ions and as-synthesized AgNPs. A visible colour change from brown to pale yellow was observed when as-synthesized AgNPs were added to 20, 1, and 0.1 mg/l  $\text{Hg}^{2+}$  solutions (Fig. 16). These findings were further supported by spectrophotometric analysis wherein, a decrease in nanoparticle SPR absorption band intensity was noted

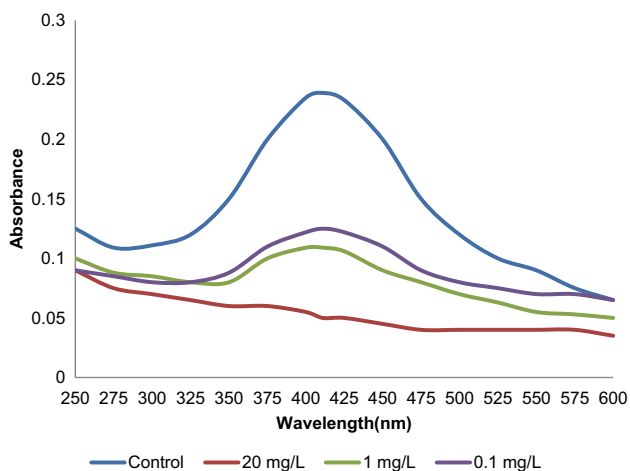


**Fig. 17** Absorption spectra of AgNPs in the presence of different  $\text{Hg}^{2+}$  ions concentrations (20 mg/l, 1 mg/l, 0.1 mg/l)

at 411 nm wavelength. This decrease in absorption band intensity highlights possible interactions between  $\text{Hg}^{2+}$  ions and AgNPs (Fig. 17). However, no colour change was observed in reaction sets with 0.01 and 0.001 mg/l  $\text{Hg}^{2+}$  ions. This indicates the lack of sensitivity of AgNPs for these  $\text{Hg}^{2+}$  concentrations. Based on these findings, the limit of  $\text{Hg}^{2+}$  detection by as-synthesized AgNPs was concluded to be 0.1 mg/l. Table 5 summarizes the limit of  $\text{Hg}^{2+}$  detection obtained in previous studies using as-synthesized AgNPs. These results show that as-synthesized AgNPs of the current study can serve as highly sensitive biosensors for selectively detecting  $\text{Hg}^{2+}$  ions.

## 4 Conclusion

In summary, the present study demonstrated that a natural renewable biomass such as cauliflower vegetable waste could be utilized as a biological source for biosynthesizing AgNPs with diverse environmental applications. The green method used for biosynthesis of AgNPs was reliable, eco-friendly, cost-effective and less time-consuming. UV-visible spectroscopy results indicated a signature absorption band for AgNPs. Further characterization revealed that the unique molecular composition of CLW extract provided the necessary reducing agents for nanoparticle synthesis. Biosynthesized AgNPs further displayed promising photocatalytic activity for degrading MB dye. These nanoparticles also demonstrated efficient colorimetric sensing ability for detecting  $\text{Hg}^{2+}$  ions. Based on these results, it can be concluded that these biosynthesized AgNPs can serve as a remarkable multipurpose tool for degrading MB dye in industrial effluents and detecting mercury based environmental pollutants.

**Acknowledgements** The authors would like to extend their gratitude to Sophisticated Analytical Instrument Facility Laboratory (SAIF) at IIT Bombay for performing FT-IR, XRD, FEG-SEM, TEM, SAED and AES. The authors would also like to thank ICAR-CIRCOT Sophisticated Analytical Instrument Facility for performing BET experiment.

**Table 5** Comparison of studies on  $\text{Hg}^{2+}$  sensing using as-synthesized AgNPs

Reducing agent for AgNP synthesis (extract)	Volume of as-synthesized AgNPs	Limit of detection of $\text{Hg}^{2+}$	References
<i>Matricaria recutita</i> (Babunah)	1 ml	49.8 $\mu\text{M}$	[21]
Soap-root plant	2 ml	2.2 $\mu\text{M}$	[67]
Burmese grape fruit	3 ml	47.60 $\mu\text{M}$	[68]
<i>Ficus carica</i> (fig) stem	100 $\mu\text{l}$	1.06 $\mu\text{M}$	[69]
Cauliflower leaf waste	100 $\mu\text{l}$	0.49 $\mu\text{M}$	Present study

## Compliance with ethical standards

**Conflict of interest** The authors declare that they have no conflict of interest.

## References

1. Prasad R (2014) Synthesis of silver nanoparticles in photosynthetic plants. *J Nanoparticles*. <https://doi.org/10.1155/2014/963961>
2. Saranya VTK, Gowrie US (2016) Photo catalytic reduction of methylene blue dye using biogenic silver nanoparticles from the aqueous cladode extract of *Casuarina equisetifolia*. *Indo Am J Pharm Res* 6:4562–4568
3. Indana MK, Gangapuram BR, Dadigala R, Bandi R, Guttena V (2016) A novel green synthesis and characterization of silver nanoparticles using gum tragacanth and evaluation of their potential catalytic reduction activities with methylene blue and congo red dyes. *J Anal Sci Technol* 7:19
4. Singh J, Kaur G, Rawat M (2016) A brief review on synthesis and characterization of copper oxide nanoparticles and its applications. *J Bioelectron Nanotechnol* 1:9
5. Parthasarathy G, Saroja M, Venkatachalam M, Shankar S, Evanjelene VK (2016) Green synthesis of zinc oxide nanoparticles—review paper. *World J Pharm Pharm Sci* 5:922–931
6. Singh J, Kukkar P, Sammi H, Rawat M, Singh G, Kukkar D (2017) Enhanced catalytic reduction of 4-nitrophenol and congo red dye by silver nanoparticles prepared from *Azadirachta indica* leaf extract under direct sunlight exposure. *Part Sci Technol* 37:1–10
7. Sengania M, Grumezescu AM, Rajeswari VD (2017) Recent trends and methodologies in gold nanoparticle synthesis—a prospective review on drug delivery aspect. *OpenNano* 2:37–46
8. Kalpana VN, Rajeswari VD (2018) A review on green synthesis, biomedical applications, and toxicity studies of ZnO NPs. *Bioinorgan Chem Appl*. <https://doi.org/10.1155/2018/3569758>
9. Veerasamy R, Xin TZ, Gunasagan S, Xiang TFW, Yang EFC, Jeyakumar N, Dhanaraj SA (2011) Biosynthesis of silver nanoparticles using mangosteen leaf extract and evaluation of their antimicrobial activities. *J Saudi Chem Soc* 15:113–120
10. Rodríguez-León E, Iñiguez-Palomares R, Navarro RE, Herrera-Urbina R, Tánori J, Iñiguez-Palomares C, Maldonado A (2013) Synthesis of silver nanoparticles using reducing agents obtained from natural sources (*Rumex hymenosepalus* extracts). *Nanoscale Res Lett* 8:318
11. Kolya H, Maiti P, Pandey A, Tripathy T (2015) Green synthesis of silver nanoparticles with antimicrobial and azo dye (Congo red) degradation properties using *Amaranthus gangeticus* Linn leaf extract. *J Anal Sci Technol* 6:33
12. Singh J, Kumar V, Jolly SS, Kim K, Rawat M, Kukkar D, Tsang YF (2019) Biogenic synthesis of silver nanoparticles and its photocatalytic applications for removal of organic pollutants in water. *J Ind Eng Chem* 80:247–257
13. Galdiero S, Falanga A, Vitiello M, Cantisani M, Marra V, Galdiero M (2011) Silver nanoparticles as potential antiviral agents. *Molecules* 16:8894–8918
14. Velusamy P, Kumar GV, Jeyanthi V, Das J, Pachaiappan R (2016) Bio-inspired green nanoparticles: synthesis, mechanism, and antibacterial application. *Toxicol Res* 32:95–102
15. Roy P, Das B, Mohanty A, Mohapatra S (2017) Green synthesis of silver nanoparticles using *Azadirachta indica* leaf extract and its antimicrobial study. *Appl Nanosci* 7:843–850
16. Vanaja M, Paulkumar K, Baburaja M, Rajeshkumar S, Gnanajobitha G, Malarkodi C, Sivakavinesan M, Annadurai G (2014) Degradation of methylene blue using biologically synthesized silver nanoparticles. *Bioinorgan Chem Appl*. <https://doi.org/10.1155/2014/742346>
17. Bonnia NN, Kamaruddin MS, Nawawi MH, Ratim S, Azlina HN, Ali ES (2016) Green biosynthesis of silver nanoparticles using *Polygonum hydropiper* and study its catalytic degradation of methylene blue. *Procedia Chem* 19:594–602
18. Jyoti K, Singh A (2016) Green synthesis of nanostructured silver particles and their catalytic application in dye degradation. *J Genet Eng Biotechnol* 14:311–317
19. Saha J, Begum A, Mukherjee A, Kumar S (2017) A novel green synthesis of silver nanoparticles and their catalytic action in reduction of Methylene Blue dye. *Sustain Environ Res* 27:245–250
20. Maiti S, Barman G, Laha JK (2016) Detection of heavy metals ( $\text{Cu}^{+2}$ ,  $\text{Hg}^{+2}$ ) by biosynthesized silver nanoparticles. *Appl Nanosci* 6:529–538
21. Uddin I, Ahmad K, Khan AA, Kazmi MA (2017) Synthesis of silver nanoparticles using *Matricaria recutita* (Babunah) plant extract and its study as mercury ions sensor. *Sens Biosens Res* 16:62–67
22. Singh J, Datta T, Kim K, Rawat M, Samddar P, Kumar P (2018) ‘Green’ synthesis of metals and their oxide nanoparticles: applications for environmental remediation. *J Nanobiotechnol* 16:84
23. Jain S, Mehata MS (2017) Medicinal plant leaf extract and pure flavonoid mediated green synthesis of silver nanoparticles and their enhanced antibacterial property. *Sci Rep* 7:15867
24. Barros CHN, Cruz GCF, Mayrink W, Tasic L (2018) Bio-based synthesis of silver nanoparticles from orange waste: effects of distinct biomolecule coatings on size, morphology, and antimicrobial activity. *Nanotechnol Sci Appl* 11:1–14
25. Singh J, Mehta A, Rawat M, Basu S (2018) Green synthesis of silver nanoparticles using sun dried tulsi leaves and its catalytic application for 4-nitrophenol reduction. *J Environ Chem Eng* 6:1468–1474
26. Khalil MMH, Ismail EH, El-Baghdady KZ, Mohamed D (2014) Green synthesis of silver nanoparticles using olive leaf extract and its antibacterial activity. *Arab J Chem* 7:1131–1139
27. Gomathi M, Rajkumar PV, Prakasam A, Ravichandran K (2017) Green synthesis of silver nanoparticles using *Datura stramonium* leaf extract and assessment of their antibacterial activity. *Resour Effic Technol* 3:280–284
28. Rónavári A, Kovács D, Igaz N, Vágvölgyi C, Boros IM, Kónya Z, Pfeiffer I, Kiricsi M (2017) Biological activity of green-synthesized silver nanoparticles depends on the applied natural extracts: a comprehensive study. *Int J Nanomed* 12:871–883
29. Vélez E, Campillo G, Morales G, Hincapié C, Osorio J, Arnache O (2018) Silver nanoparticles obtained by aqueous or ethanolic *Aloe vera* extracts: an assessment of the antibacterial activity and mercury removal capability. *J Nanometer*. <https://doi.org/10.1155/2018/7215210>
30. Sharma K, Kaushik S, Jyoti A (2016) Green synthesis of silver nanoparticles by using waste vegetable peel and its antibacterial activities. *J Pharm Sci Res* 8:313–316
31. Mythili R, Selvankumar T, Kamala-Kannan S, Sudhakar C, Ameen F, Al-Sabri A, Selvam K, Govarthanan M, Kim H (2018) Utilization of market vegetable waste for silver nanoparticle synthesis and its antibacterial activity. *Mater Lett* 225:101–104
32. Patel R, Mehta M (2019) Green synthesis of silver nanoparticles by using fruit and vegetable waste: a review. *Int J Eng Res Appl* 9:78–85
33. Khedkar MA, Nimbalkar PR, Chavan PV, Chendake YJ, Bankar SB (2017) Cauliflower waste utilization for sustainable biobutanol

- production: revelation of drying kinetics and bioprocess development. *Bioprocess Biosyst Eng* 40:1493–1506
34. Cartea ME, Francisco M, Soengas P, Velasco P (2011) Phenolic compounds in *Brassica* vegetables. *Molecules* 16:251–280
  35. Sridhara V, Pratima K, Krishnamurthy G, Sreekanth B (2013) Vegetable assisted synthesis of silver nanoparticles and its antibacterial activity against two human pathogens. *Asian J Pharm Clin Res* 6:53–57
  36. Tamileswari R, Nisha MH, Jesurani SS (2015) Analysis of antimicrobial activity silver nanoparticle from the Brassicaceae family vegetables. *Int J Eng Sci Res Technol* 4:804–811
  37. Singh A, Sharma B, Deswal R (2018) Green silver nanoparticles from novel Brassicaceae cultivars with enhanced antimicrobial potential than earlier reported Brassicaceae members. *J Trace Elem Med Biol* 47:1–11
  38. Ranjitham M, Suja R, Caroling G, Tiwari S (2013) *In vitro* evaluation of antioxidant, antimicrobial, anticancer activities and characterisation of *Brassica oleracea*. Var. *Bortrytis*. L synthesized silver nanoparticles. *Int J Pharm Pharm Sci* 5:239–251
  39. Balu S, Uma K, Pan G, Yang TCK, Ramaraj SK (2018) Degradation of methylene blue dye in the presence of visible light using  $\text{SiO}_2/\alpha\text{-Fe}_2\text{O}_3$  nanocomposites deposited on  $\text{SnS}_2$  flowers. *Materials* 11:1030
  40. Mavaei Mavaei M, Chahardoli A, Shokoohinia Y, Khoshroo A, Fattahi A (2020) One-step synthesized silver nanoparticles using isoimperatorin: evaluation of photocatalytic, and electrochemical activities. *Sci Rep* 10:1762
  41. Gayda GZ, Demkiv OM, Stasyuk NY, Serkiz RY, Lootsik MD, Errachid A, Gonchar MV, Nisnevitch M (2019) Metallic nanoparticles obtained via “green” synthesis as a platform for biosensor construction. *Appl Sci* 9:720
  42. Umadevi M, Shalini S, Bindhu MR (2012) Synthesis of silver nanoparticle using *D. carota* extract. *Adv Nat Sci Nanosci Nanotechnol* 3:025008
  43. Kumari M, Mishra A, Pandey S, Singh SP, Chaudhry V, Mudiam MKR, Shukla S, Kakkar P, Nautiyal CS (2016) Physico-chemical condition optimization during biosynthesis lead to development of improved and catalytically efficient gold nano particles. *Sci Rep* 6:27575
  44. Pal J, Deb MK, Deshmukh DK (2014) Microwave-assisted synthesis of silver nanoparticles using benzo-18-crown-6 as reducing and stabilizing agent. *Appl Nanosci* 4:507–510
  45. Verma A, Mehata MS (2016) Controllable synthesis of silver nanoparticles using Neem leaves and their antimicrobial activity. *J Rad Res Appl Sci* 9:109–115
  46. Chowdhury A, Kunjiappan S, Bhattacharjee C, Chowdhury R (2014) Green synthesis and characterization of biocompatible silver nanoparticles using *Brassica oleracea* L. leaf extract. *Int J Curr Res* 6:6166–6174
  47. Balashanmugam P, Kalaichelvan PT (2015) Biosynthesis characterization of silver nanoparticles using *Cassia roxburghii* DC. aqueous extract, and coated on cotton cloth for effective antibacterial activity. *Int J Nanomed* 10:87–97
  48. Pirtarighat S, Ghannadnia M, Baghshahi S (2019) Green synthesis of silver nanoparticles using the plant extract of *Salvia spinosa* grown in vitro and their antibacterial activity assessment. *J Nanostruct Chem* 9:1–9
  49. Anandalakshmi K, Venugobal J, Ramasamy V (2016) Characterization of silver nanoparticles by green synthesis method using *Petalium murex* leaf extract and their antibacterial activity. *Appl Nanosci* 6:399–408
  50. de Jesús Ruíz-Baltazara Á, Reyes-López SY, de Lourdes Mondragón-Sánchez M, Estevez M, Hernández-Martínez AR, Pérez R (2018) Biosynthesis of Ag nanoparticles using *Cynara cardunculus* leaf extract: evaluation of their antibacterial and electrochemical activity. *Results Phys* 11:1142–1149
  51. Ajitha B, Reddy AKY, Reddy PS (2015) Green synthesis and characterization of silver nanoparticles using *Lantana camara* leaf extract. *Mater Sci Eng C* 49:373–381
  52. Guan B, Fan L, Wu X, Wang P, Qiu Y, Wang M, Guo Z, Zhang N, Sun K (2018) The facile synthesis and enhanced lithium–sulfur battery performance of an amorphous cobalt boride ( $\text{Co}_2\text{B}$ )@graphene composite cathode. *J Mater Chem A* 6:24045–24049
  53. Elzey S, Grassian VH (2010) Agglomeration, isolation and dissolution of commercially manufactured silver nanoparticles in aqueous environments. *J Nanopart Res* 12:1945–1958
  54. Zhou M, Wei Z, Qiao H, Zhu L, Yang H, Xia T (2009) Particle size and pore structure characterization of silver nanoparticles prepared by confined arc plasma. *J Nanomater* 2009:5
  55. Joshi SJ, Geetha SJ, Al-Mamari S, Al-Azkawi A (2018) Green synthesis of silver nanoparticles using pomegranate peel extracts and its application in photocatalytic degradation of methylene blue. *Jundishapur J Nat Pharm Prod* 13:e67846
  56. Sumitha S, Vasanthi S, Shalini S, Chinni SV, Gopinath SCB, Anbu P, Bahari MB, Harish R, Kathiresan S, Ravichandran V (2018) Phyto-mediated photo catalysed green synthesis of silver nanoparticles using *Durio zibethinus* seed extract: antimicrobial and cytotoxic activity and photocatalytic applications. *Molecules* 23:3311
  57. Chandraker SK, Lal M, Shukla R (2019) DNA-binding, antioxidant,  $\text{H}_2\text{O}_2$  sensing and photocatalytic properties of biogenic silver nanoparticles using *Ageratum conyzoides* L. leaf extract. *RSC Adv* 9:23408–23417
  58. Kumar MS, Supraja N, David E (2019) Photocatalytic degradation of methylene blue using silver nanoparticles synthesized from *Gymnema sylvestre* and antimicrobial assay. *Nov Res Sci* 2:1–7
  59. Allibone J, Fatemian E, Walker PJ (1999) Determination of mercury in potable water by ICP-MS using gold as a stabilising agent. *J Anal At Spectrom* 14:235–239
  60. Ghaedi M, Fathi MR, Shokrollahi A, Shajarat F (2006) Highly selective and sensitive preconcentration of mercury ion and determination by cold vapor atomic absorption spectroscopy. *Anal Lett* 39:1171–1185
  61. Wang H, Wang Y, Jin J, Yang R (2008) Gold nanoparticle-based colorimetric and “turn-on” fluorescent probe for mercury(II) ions in aqueous solution. *Anal Chem* 80:9021–9028
  62. Gupta S, Singh R, Anoop MD, Kulshrestha V, Srivastava DN, Ray K, Kothari SL, Awasthi K, Kumar M (2018) Electrochemical sensor for detection of mercury (II) ions in water using nanostructured bismuth hexagons. *Appl Phys A* 124:737
  63. Jeevika A, Shankaran DS (2016) Functionalized silver nanoparticles probe for visual colorimetric sensing of mercury. *Mater Res Bull* 83:48–55
  64. Prasad KS, Shruthi G, Shivamallu C (2018) Functionalized silver nano-sensor for colorimetric detection of  $\text{Hg}^{2+}$  ions: facile synthesis and docking studies. *Sensors* 18:2698
  65. Firdaus LM, Fitriani I, Wyantuti S, Hartati YW, Renat K, Mcalister JA, Obata TG (2017) Colorimetric detection of mercury (II) ion in aqueous solution using silver nanoparticles. *Anal Sci* 33:831–837
  66. Tanvir F, Yaqub A, Tanvir S, Ran A, Anderson WA (2019) Colorimetric detection of mercury ions in water with capped silver nanoprisms. *Materials (Basel)* 12:1533
  67. Farhadia K, Forougha M, Molaeia R, Hajizadeha S, Rafipour A (2012) Highly selective  $\text{Hg}^{2+}$  colorimetric sensor using green synthesized and unmodified silver nanoparticles. *Sens Actuators B* 161:880–885
  68. Alam MN, Chatterjee A, Das S, Batuta S, Mandal D, Begum NA (2015) Burmese grape fruit juice can trigger the “logic gate”-like colorimetric sensing behavior of Ag nanoparticles towards toxic metal ions. *RSC Adv* 5:23419–23430

69. Kalam A, Al-Sehemi GS, Alrumman S, Assiri M, Moustafa MFM, Yadav P, Pannipara M (2018) Colorimetric optical chemosensor of toxic metal ion ( $\text{Hg}^{2+}$ ) and biological activity using green synthesized AgNPs. *Green Chem Lett Rev* 11:484–491

**Publisher's Note** Springer Nature remains neutral with regard to jurisdictional claims in published maps and institutional affiliations.